Structural, electronic and magnetic properties of Gd investigated by DFT+*U* methods: bulk, clean and H-covered (0001) surfaces

2006 J. Phys.: Condens. Matter 18 7021

(http://iopscience.iop.org/0953-8984/18/30/007)

INSTITUTE OF PHYSICS PUBLISHING JOURNAL OF PHYSICS: CONDENSED MATTER

J. Phys.: Condens. Matter **18** (2006) 7021–7043 doi:10.1088/0953-8984/18/30/007

Structural, electronic and magnetic properties of Gd investigated by DFT + U methods: bulk, clean and H-covered (0001) surfaces

Melissa Petersen[1], **Jürgen Hafner and Martijn Marsman**

Institut für Materialphysik and Center for Computational Materials Science, Universität Wien, Sensengasse 8/12, A-1090 Wien, Austria

E-mail: melissa@science.uct.ac.za, juergen.hafner@univie.ac.at and martijn.marsman@univie.ac.at

Received 27 April 2006, in final form 26 June 2006
Published 14 July 2006
Online at stacks.iop.org/JPhysCM/18/7021

Abstract

The structural, electronic and magnetic properties of bulk Gd and of the Gd(0001) surface have been investigated using *ab initio* calculations based on density-functional theory (DFT) and on DFT + U calculations. In agreement with earlier work we find that the neglect of the strong correlation of the 4f electrons leads to the wrong prediction of an antiferromagnetic ground state of hexagonal close-packed (hcp) Gd, as well as to substantial errors in the magnetic moments and exchange splitting. If the strong on-site Coulomb repulsion in the 4f band is described by a Hubbard-like term added to the DFT Hamiltonian, an improved description of the structural, electronic and magnetic properties of both bulk Gd and of the Gd(0001) surface is achieved. The enhancement of the exchange coupling and of the magnetic ordering temperature at the surface is investigated using a simple model. The adsorption of hydrogen on the Gd(0001) surface and its diffusion into deeper layers has been investigated. It is shown that H adsorption eliminates the electronic surface state which is partly responsible for the enhanced magnetism at the clean surface and leads to the formation of H-induced electronic states below the bottom of the valence band.

1. Introduction

The rare-earth ferromagnet gadolinium has been the subject of extensive theoretical investigation. Gd is characterized by a fully spin-polarized half-filled 4f shell. By Hund's rules, occupation of the 4f states leads to a high spin-derived contribution to the magnetic moment and a vanishing orbital moment ($S = \frac{7}{2}$, $L = 0$). Since the 4f states are highly localized with negligible overlap, the 4f moments are coupled via a Ruderman–Kittel–Kasuya–Yosida

[1] Present address: Department of Chemistry, University of Cape Town, Rondebosch, 7701, Cape Town, South Africa.

(RKKY)-type exchange which is mediated by the valence electrons. The 4f moments lead to an induced polarization of the 6s and 5d valence electrons, resulting in a measured magnetic moment per atom of $7.63 \pm 0.01\ \mu_B$ [1].

The correct description of the highly localized 4f states in Gd presents a challenge for *ab initio* electronic structure calculations. The failure of the local spin-density approximation (LSDA) to successfully describe the structural, electronic and magnetic properties of bulk Gd is now well documented. Singh [2] performed calculations using the LSDA within a full-potential linearized augmented plane wave (LAPW) scheme, treating the 4f electrons as itinerant states. Agreement of the calculated structural properties with experiment was concluded to be 'fair at best'. Calculation of the band structure yielded a majority-spin 4f manifold centred at 4.5 eV below the Fermi energy (E_F) and a minority-spin 4f manifold centred at 0.5 eV above E_F, respectively, as was similarly noted in other studies [3–8]. This is in contrast to the available spectroscopic experiments which place the occupied 4f states at approximately 8 eV below E_F using x-ray photoemission spectroscopy (XPS), and the unoccupied 4f states at approximately 4.4 eV above E_F as determined with inverse photoemission spectroscopy (IPES) (also known as Bremsstrahlung isochromat spectroscopy (BIS)) [9, 10].

A closely related problem is the correct prediction of the magnetic ground state of bulk Gd. Heinemann and Temmerman [11, 12] found that the LSDA favours antiferromagnetic over ferromagnetic order when the 4f electrons are treated as valence band states, in contradiction to experiment. This was confirmed in a number of subsequent studies [6, 13–16]. The application of gradient corrections, as proposed by Langreth, Mehl and Hu [17, 18], to the exchange–correlation functional led to the prediction of the correct ferromagnetic ground state in linearized muffin tin orbital (LMTO) calculations employing the atomic sphere approximation (ASA) [11]. Although Jenkins *et al* [14] obtained the same result using the LMTO-ASA approach with both the generalized gradient approximations (GGA) of Perdew and Wang (PW91) [19] and of Perdew, Burke and Ernzerhof (PBE) [20], they found that the antiferromagnetic state was once again favoured when a full-potential (FP)-LMTO method was used instead. This result was consistent with previous FP-LMTO calculations [13] and subsequent full-potential linearized augmented-plane wave (FLAPW) calculations [6] using the PW91 functional when treating the 4f electrons as valence band states. Kurz *et al* [6] argued that the favouring of the antiferromagnetic ground state could be traced back to the overestimation of the itinerancy of the 4f states by the LSDA and GGA, which results in an unphysical contribution of the minority-spin 4f electrons to the density of states at the Fermi level. Thus, theoretical models which have the effect of removing the 4f electron states from the vicinity of the Fermi level should obtain the correct ferromagnetic ground state.

One approach which has the effect of restoring the correct magnetic ground state is to treat the 4f electrons as core states rather than itinerant band states. In effect, this removes the hybridization of the unoccupied 4f electrons with the valence 6s, 6p and 5d electrons. Sticht and Kübler [5] argued against a treatment of the 4f electrons as core states, on the grounds that it resulted in an induced spin moment due to the conduction electrons that was unacceptably higher than experiment. However, Richter and Eschrig [21] subsequently questioned the validity of their calculated magnetic moment, preferring a model in which the 4f electrons are treated as localized states. Singh [2] concluded that the 4f electrons had to be treated as itinerant states rather than core states in order to allow for the (s, d)-f hybridization needed to reproduce the complexity of the Fermi surface, but this claim was refuted by Ahuja *et al* [22]. Eriksson *et al* [13] demonstrated that the 4f-core model leads to the correct ferromagnetic ground state in both LSDA and GGA [19] calculations, a claim which was verified by Kurz *et al* [6, 23]. In these calculations, the minority-spin contribution of the 4f electrons to the density of states at E_F is removed, either directly [6] or indirectly [13].

In a series of studies on Gd, Bylander and Kleinman [24–26] argued that the appearance of the minority-spin 4f manifold just above E_F in the calculated bulk Gd band structure is an artefact of the DFT (both in the LSDA and in the GGA). In their calculations, they took an alternative approach, in which a Hartree–Fock exchange potential was used to describe the interaction between the valence and core electrons, with an LSDA exchange potential for the interaction of the valence electrons amongst themselves. A single adjustable parameter was introduced to obtain the correct experimental magnetization. The majority-spin 4f states were treated as localized core electrons, while the minority-spin 4f states were treated within the band Hamiltonian. In this approach, the correct ferromagnetic ground state is obtained, [25] and the minority-spin 4f bands are successfully shifted away from the Fermi level, resulting in a concomitant reduction in the density of states at E_F. However, the minority-spin 4f manifold is found to be located at much higher energies (above 8.36 eV) than obtained in BIS measurements [9] (4.4 eV).

Part of the failure of the LSDA to correctly describe the properties of Gd has been attributed to the so-called self-interaction problem [27], which is particularly significant for strongly correlated systems with localized states. In the LSDA, the approximate nature of the exchange–correlation energy functional leads to incomplete cancellation of the Coulomb interaction of an electron with itself by the exchange interaction. Application of self-interaction-corrected (SIC) functionals to rare-earth systems has led to improvements in the description of these materials. Temmerman *et al* [28] applied the SIC–LSDA scheme to the treatment of the rare-earth metal praseodymium. The effect of the SIC was to split the 4f band into occupied and unoccupied manifolds, both located far away from the Fermi level. Their SIC–LSDA approach was successfully applied to the treatment of a range of other rare-earth systems, [29] which included Gd in a study of valency relationships in rare earths and their compounds [30].

A further approach which has been advocated in the treatment of strongly correlated systems with localized 4f states is the LDA + U method [31–34]. In this approach, a Hubbard-like term is added to the DFT Hamiltonian to account for the strong on-site intra-atomic Coulomb repulsion U between the electrons occupying the localized 4f states in the lanthanides or the narrow 3d band in transition-metal compounds. The LDA + U approach applied to Gd has the effect of shifting both the majority- and minority-spin 4f states away from the Fermi level [3, 6, 15, 16], reducing the density of states at E_F [15], and leading to a correct ferromagnetic ground state [6, 15, 16].

A problem closely related to the character of the 4f states and to the magnitude of the magnetic energy difference between the ferromagnetic (FM) and antiferromagnetic (AFM) states is the magnetic properties at finite temperature and the prediction of the Curie temperature for ferromagnetic ordering. Turek *et al* [23] have used a treatment based on a Heisenberg Hamiltonian with long-range exchange-pair interactions derived from the self consistent electronic structure of the FM ground state using the magnetic force theorem [35]. The electronic structure has been calculated in the LSDA using the LMTO-ASA and the 4f-core model, and the Curie temperature is determined in a mean-field approximation. The resulting Curie temperature is only 14% above the experimental value, but in view of all the approximations entering this approach (neglect of gradient corrections, atomic sphere approximation, frozen 4f states, mean-field model) this degree of agreement must be considered as largely coincidental. This statement is further supported by the fact that an even simpler mapping procedure, based only on nearest-neighbour exchange interactions derived from the energy difference between the FM and AFM states, achieves as good agreement with experiment. An alternative approach to the temperature-dependent magnetism of Gd based on a combination of many-body interactions with band-structure calculations has been presented by Nolting *et al* [4, 36]. This approach predicts a temperature behaviour which strongly depends

on the degree of itinerancy of the corresponding electronic eigenstates and their hybridization with the 4f states. The weakly correlated s states display a temperature dependence consistent with a Stoner-like band picture and a collapse of the exchange splitting at the Curie temperature (consistent with the photoemission data of Kim *et al* [37]), while for the more localized d-like states a persisting exchange splitting in the paramagnetic phase is possible. Evidence for such a behaviour is provided by spin-resolved photoemission experiments of Maiti *et al* [38]. Very recently Khmelevskyi *et al* [39] have used the disordered local moment (DLM) formalism to study the magnetic splitting of the (s, d) valence-band induced by the 4f moments. They report that the local exchange splitting persists above T_C, in agreement with the experimental findings of Maiti *et al*. The conclusion is that the magnetism of Gd is too complex to allow for a description in terms of core-like 4f states decoupled from the Stoner-like s, d states.

The unusual character of the magnetism of the Gd(0001) surface adds to the complexity of the problem. The results of various spectroscopic measurements suggest a significant enhancement of the surface Curie temperature T_C^s compared to the bulk value [40–44]. However, the existence of a surface phase transition decoupled from the magnetic transition in the bulk remains controversial. On the basis of surface magnetization measurements using spin-polarized secondary-electron emission spectroscopy and bulk magnetization measurements using the magneto-optic Kerr effect, Arnold and Pappas [45] concluded that the surface undergoes an ordinary phase transition, i.e. at a common Curie temperature for surface and bulk. On the basis of a comparison of spin-polarized low-energy electron diffraction (LEED) and magnetic–optic Kerr effect measurements, even a possible AFM alignment of the moments in the surface layer with respect to the FM bulk was suggested [41]. However, more recent core and valence PES experiments failed to confirm this AFM alignment and demonstrated that at least the in-plane component of the surface magnetization is parallel to the bulk [42, 44, 46–48]. However, the possibility of a canted magnetic structure at the surface is not excluded [49]. Core-level PES experiments on bulk-like, 300 Å thick Gd/W(110) films show spin asymmetries well above the bulk T_C and suggest a surface-induced enhancement of T_C^s of as much as 85 K. LEED experiments [50, 51] agree on an inward relaxation of the surface layer and an expansion of the distance between the subsurface layer and the bulk. However, Quinn *et al* [51] report significantly larger d relaxations than Giergiel *et al* [50]. A first electronic structure study of the Gd(0001) surface by Wu *et al* [52] predicted an outward relaxation of the surface layer and an AFM coupling between bulk and surface, in contradiction to experiment. A subsequent FP-LMTO study by Eriksson *et al* [13] using the LSDA and the 4f-core model calculated a slightly larger inward relaxation than found in the experiment, and predicted a FM coupling between bulk and surface and an enhanced 5d contribution to the magnetic moment at the surface. However, they stopped short of evaluating the surface Curie temperature. Shick *et al* [53] used the LDA+U and the experimentally determined surface structure in their FLAPW calculations. For the relaxed surface they found an enhanced 5d moment and an energy difference $\Delta E(\downarrow\uparrow - \uparrow\uparrow)$ between AFM and FM coupled surface layers which is substantially larger than the magnetic energy difference $\Delta E(\mathrm{AFM} - \mathrm{FM})$ in the bulk. The ratio between these two energy differences was considered as a measure for the difference between the exchange coupling at the free surface and in the bulk, $J_s/J_b = \Delta E(\downarrow\uparrow - \uparrow\uparrow)/\Delta E(\mathrm{AFM} - \mathrm{FM})$. Within a mean-field model, this leads to $T_c^s = 1.33 \times T_c$, in good agreement with experiment. More recently, FLAPW investigations of the Gd(0001) surface using both the 4f-core and 4f-band models and the LDA + U have been presented by Kurz *et al* [6]. The results show that the inward relaxation of the surface is equally well described by both the 4f-core and 4f-band models, while the band model produces no and the 4f-core model only a modest surface-induced enhancement of the magnetic moments. Using the 4f-core model Kurz *et al* [6] calculate a ratio $\Delta E(\downarrow\uparrow - \uparrow\uparrow)/\Delta E(\mathrm{AFM} - \mathrm{FM}) \sim 1.92$, corresponding to a T_C-enhancement by 21%.

Calculations using the LDA + U have been performed only for the surface geometry derived using the 4f-core model and predict a ratio of $\Delta E(\downarrow\uparrow - \uparrow\uparrow)/\Delta E(\mathrm{AFM} - \mathrm{FM}) \sim 2.79$ and hence a very large T_C-enhancement of 61%. Given the fact that both calculations used the same electronic structure method and the same value for the on-site Coulomb potential, the difference between the results of Shick *et al* [53] and Kurz *et al* [6] is rather disappointing. Kurz *et al* [6] attribute this discrepancy to different muffin-tin radii used in the construction of the FLAPW basis and potential.

It is well known that adsorbates can significantly alter the electronic and magnetic properties of the underlying substrate. Hydrogen adsorption on rare-earth surfaces is strongly temperature dependent: at low temperatures, H is adsorbed dissociatively on the surface, but dissolves into the bulk on moderate heating. Early experiments by Cerri *et al* [54] reported a drastic reduction of the spin polarization and the magnetic ordering temperature induced by hydrogen adsorption. Photoemission experiments by Li *et al* [55] report a strong attenuation of the surface state near E_F characteristic for the clean Gd(0001) surface and the appearance of two H-induced states at -3.8 and -6 eV below the Fermi edge. LEED experiments show that there is no H-induced surface reconstruction: the surface periodicity remains (1×1) at all coverages. Recently, H adsorption on Gd(0001) has been studied intensely by Getzlaff *et al* [56–58] by a combination of STM and PES experiments. The strong hydrogen-induced suppression of the surface state and the formation of a H-induced state at ~ -4 eV was confirmed, whereas in these low-temperature studies the H-induced feature at -6 eV has only very low intensity.

In this paper we present our results of *ab initio* investigations of the structural, electronic and magnetic properties of bulk Gd and of clean and H-covered Gd(0001) surfaces, using both DFT and DFT + U calculations. We demonstrate that the Hubbard correction for the on-site Coulomb repulsions not only corrects the exchange splitting of the 4f states, but also leads to an improved description of the induced magnetization of the valence states. In addition, we present DFT + U calculations for clean and H-covered Gd(0001) surfaces.

2. Methodology

The investigations described in the present work have been performed using the Vienna *ab initio* simulation package, VASP [59–63]. VASP performs an iterative solution of the Kohn–Sham equations of DFT using a plane-wave basis and the projector augmented wave (PAW) method [64] in the implementation of Kresse and Joubert [63] to describe the electron–ion interaction. The calculations have been performed in a scalar-relativistic mode, neglecting spin–orbital coupling. Test calculations have shown (in agreement with earlier studies) that the orbital moment is very small and that the inclusion of the spin–orbit term leads to negligible changes in the results. For the construction of the PAW potentials, the 5s and 5p semicore states have been treated as valence electrons (i.e. we have 18 valence electrons per Gd atom). Treating the 5s and 5p orbitals as valence states greatly improves the description of the valence–core exchange interaction. The cut-off energy for the plane-wave basis set was 333 eV for bulk calculations and for the investigation of the clean Gd(0001) surface. For the study of the hydrogen-covered surface, the cut-off was reduced to 256.5 eV to save computer time. Test calculations for bulk Gd show that this reduction of the cut-off hardly influences the results.

At the level of the LSDA, the exchange–correlation functional proposed by Perdew and Zunger [27] (based on the quantum Monte Carlo calculations of Ceperley and Alder [65]), together with the spin interpolation proposed by Vosko *et al* [66] was used. At the GGA level, the semilocal functional proposed by Perdew, Burke and Ernzerhof (PBE) [20] has been used. The influence of the generalized gradient corrections (GGCs) on the results of calculations of physical properties is by now well documented (see, e.g. Moroni *et al* [67]

and further references given therein). (i) They correct the overbinding tendency characteristic for the LSDA, leading to smaller cohesive energies and larger equilibrium lattice constants. (ii) For magnetic systems, GGCs predict a slightly enhanced exchange splitting and larger magnetic moments. Generally, the magnetic state is stabilized relative to the non-magnetic state. (iii) For adsorption at metallic surfaces, the LSDA predicts in many cases a qualitatively incorrect potential-energy surface, whereas the SGGA results in a correct description of the adsorption/desorption dynamics [68, 69].

The DFT + U approach used here is based on the work of Dudarev *et al*, [34] using a model Hamiltonian of the form [34]

$$\hat{H} = \frac{U}{2} \sum_{m,m',\sigma} \hat{n}_{m,\sigma} \hat{n}_{m',-\sigma} + \frac{(U-J)}{2} \sum_{m \neq m',\sigma} \hat{n}_{m,\sigma} \hat{n}_{m',\sigma} \tag{1}$$

where $\hat{n}_{m\sigma}$ is the operator yielding the number of electrons occupying an orbital with magnetic quantum number m and spin σ at a particular site. The Coulomb repulsion is characterized by a spherically averaged Hubbard parameter U describing the energy increase for placing an extra electron into the 4f level on a particular site, $U = E(4f^{n+1}) + E(4f^{n-1}) - 2E(4f^n)$, and a parameter J representing the screened exchange energy. While U depends on the spatial extension of the wavefunctions and on screening, J is an approximation to the Stoner exchange parameter and is almost constant, $J \sim 1$ eV. The Mott–Hubbard Hamiltonian includes energy contributions already accounted for by the DFT functional. To correct for this 'double counting', equation (1) is estimated in the limit of integer occupancies and subtracted from the DFT energy to obtain the spin-polarized DFT + U energy functional [34, 70]. A simple functional is obtained after some straightforward algebra [34]:

$$E_{\mathrm{DFT}+U} = E_{\mathrm{DFT}} + \frac{U-J}{2} \sum_{m\sigma} (\hat{n}_{m\sigma} - \hat{n}^2_{m\sigma}). \tag{2}$$

This energy functional is not yet invariant with respect to a unitary transformation of the orbitals. A formulation given by Liechtenstein *et al* [33] replaces the number operator by the on-site density matrix ρ^σ_{ij} of the 4f electrons to obtain a rotationally invariant energy functional. In the present case this yields the functional [34]

$$E_{\mathrm{DFT}+U} = E_{\mathrm{DFT}} + \frac{U-J}{2} \sum_{\sigma} \mathrm{Tr}[\rho^\sigma - \rho^\sigma \rho^\sigma]. \tag{3}$$

The interpretation of this DFT + U functional is particularly simple. In the limit of an idempotent on-site occupancy matrix ρ^σ

$$\rho^{\sigma\,2} = \rho^\sigma,$$

the DFT + U functional yields exactly the same energy as the DFT functional $E_{\mathrm{DFT}+U} = E_{\mathrm{DFT}}$. If $U > J$, the second term in equation (3) can be interpreted as a positive-definite penalty function driving the on-site occupancy matrices towards idem-potency: the 'strength' of the penalty function is parameterized by a *single* parameter $U - J$. The local one-electron potential given by the functional derivative of the total energy with respect to the electron density,

$$V^\sigma_{ij} = \frac{\delta E_{\mathrm{DFT}+U}}{\delta \rho^\sigma_{ij}} = \frac{\delta E_{\mathrm{DFT}}}{\delta \rho^\sigma_{ij}} + (U-J)\left[\frac{1}{2}\delta_{ij} - \rho^\sigma_{ij}\right], \tag{4}$$

is lowered for filled 4f orbitals which are localized on one particular site by $-(U-J)1/2$, whereas empty 4f orbitals are raised to higher energies by $(U-J)1/2$. The implementation of the DFT + U formalism in the PAW method has been described in detail by Bengone *et al* [71] and Rohrbach *et al* [72]. The crucial link between the PAW and the DFT + U method is the identification of the on-site density matrix ρ^σ with the PAW on-site density matrix.

Table 1. Calculated structural and magnetic properties for ferromagnetic (FM) and antiferromagnetic (AFM) bulk hcp Gd determined using the PBE + U and the PBE methods. The PBE + U results were calculated with $(U - J) = 6$ eV.

Method	V/atom (Å^3)	a (Å)	c (Å)	c/a	B (GPa)	M (μ_B)	ΔE(AFM − FM) (meV/atom)
PBE + U							
FM	32.96	3.62	5.80	1.60	35.6	+7.64	0
AFM	32.95	3.59	5.91	1.65	35.8	±7.58	69
PBE							
FM	33.59	3.65	5.82	1.60	34.9	+7.44	0
AFM	32.85	3.62	5.79	1.60	34.6	±7.35	−7
Expt.[a]	33.05	3.629 ± 0.002	5.796 ± 0.004	1.597	39.1, 41.3	+7.63 ± 0.01	>0

[a] Lattice parameters taken at 106 K from [77]. Bulk moduli extrapolated to 0 K derived from measured elastic constants (41.3 GPa) [78, 79] and acoustic sound velocity measurements (39.1 GPa) [79, 80]. Magnetic moment from [1].

Further details of the calculations are as follows. Brillouin-zone calculations are based on Γ-centred Monkhorst–Pack [73] meshes, using a modest Methfessel–Paxton [74] first-order smearing with $\sigma = 0.1$ eV. For bulk Gd, a $16 \times 16 \times 9$ grid was used. The Gd(0001) surfaces have been modelled by symmetric eight-layer slabs, allowing two layers on both sides to relax and using a $16 \times 16 \times 1$ grid for Brillouin-zone integrations. For exploring the potential-energy surface of hydrogen atoms on the Gd(0001) surface, a thinner six-layer slab with a 2×2 surface periodicity and an $8 \times 8 \times 1$ grid was used. We have verified that the reduced set-up changes the work function by only 0.02 eV. Optimization of the geometry of the hexagonal unit cell of Gd, surface relaxation and the optimization of the geometric structure of the adsorbate–substrate complex have been performed by using the Hellmann–Feynman forces and a conjugate-gradient total-energy minimization. The equilibrium lattice constant and the bulk modulus have been determined by fitting the total energy as a function of volume by a Murnaghan equation of state [75]. Magnetic moments for bulk Gd were calculated by integrating the spin-polarized DOS up to the Fermi level. Local magnetic moments have been calculated by projecting the plane-wave components of the spin-polarized eigenstates onto spherical waves within overlapping atomic spheres, with atomic radii derived from the equilibrium atomic volume (see table 1). We have verified that for the bulk both approaches lead to results in good agreement with each other.

3. Properties of hcp gadolinium

In the following we present our results for bulk hcp Gd calculated using the DFT in the generalized gradient approximation of Perdew, Burke and Ernzerhof (PBE) [20] and using the DFT + U method. Although attempts [15] have been made to calculate the on-site Coulomb potential U *a priori*, it is essentially an empirical parameter. Many previous DFT + U calculations suffer from the drawback that different values of U are needed to bring different physical properties into agreement with experiment. This is true particularly if the DFT + U calculations are based on an LSDA Hamiltonian. Rohrbach *et al* [72, 76] have demonstrated that these divergencies can be greatly reduced if the on-site Hubbard corrections are added to a GGA Hamiltonian. In the following we adopt this approach and we begin by determining the optimal value of $(U - J)$ in GGA-PBE + U calculations.

3.1. $(U - J)$ parameter fitting

Gd crystallizes in the hexagonal close-packed (hcp) structure, with lattice parameters of $a = 3.629$ Å, $c = 5.796$ Å and a c/a ratio of 1.597 [77]. Values for the bulk modulus,

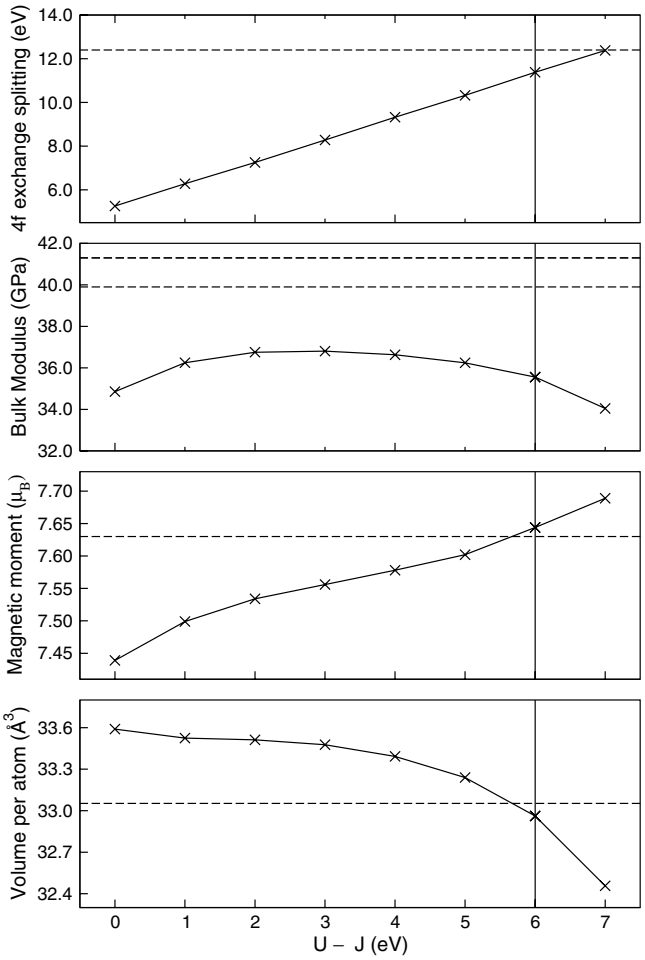

Figure 1. Calculated exchange splitting of the 4f states, bulk modulus, magnetic moment and atomic volume of ferromagnetic bulk Gd as a function of $(U - J)$ within the PBE + U method, using the PBE [20] functional. Experimental values are indicated by the horizontal dashed line in each case. The vertical line corresponds to $(U - J) = 6$ eV.

determined at low temperature (4.2 K) and extrapolated to 0 K, are 41.3 GPa, obtained from measured single-crystal elastic constants, [78, 79] and 39.9 GPa, determined by acoustic sound velocity measurements of polycrystalline Gd [79, 80]. The saturated magnetic moment is 7.63 ± 0.01 μ_B [1], with a corresponding ferromagnetic bulk Curie temperature of 293.4 K [81].

As a first step to calculating the ground state structural, electronic and magnetic properties of ferromagnetic Gd metal, the variation of the calculated equilibrium volume, bulk modulus, magnetic moment and exchange splitting of the majority- and minority-spin 4f states was investigated as a function of the U and J parameters used in the PBE + U approach (figure 1). We note that within the implementation of Dudarev *et al* [34] used here, the calculated properties depend only on the difference $(U-J)$ between the Coulomb and exchange parameters. The exchange parameter, J, was therefore fixed at 1 eV and the Coulomb interaction, U, was varied from 1 to 8 eV. A value of $U - J = 0$ eV corresponds to a standard DFT calculation with the PBE exchange–correlation energy functional.

It is immediately apparent in figure 1 that an increase in $(U - J)$ leads to improved agreement between the calculated and experimental properties for all but the bulk modulus. The calculated equilibrium volume/atom for ferromagnetic Gd is observed to decrease with increasing $(U - J)$ from 33.59 Å^3 in the PBE approach ($U - J = 0$ eV), reaching the experimental [77] volume/atom of 33.05 Å^3 at a $(U - J)$ value close to 6 eV. A similar improvement in the magnetic moment is obtained, once again reaching agreement with the experimental magnetic moment of 7.63 ± 0.01 μ_B for $(U - J)$ slightly less than 6 eV. The bulk modulus varies only weakly with the on-site potential, reaching a maximum value of 36.8 GPa at $(U - J) = 3$ eV, which underestimates by 8% the lower value of the bulk modulus, 39.9 GPa, determined by Rosen [80]. The calculated bulk modulus is then seen to decrease on further increase of $(U - J)$, leading to progressively poorer agreement with experiment. We note, however, that the reported bulk moduli, calculated using a variety of different theoretical approaches, range from 35.0 GPa, obtained with the LMTO-ASA method and using generalized gradient corrections [11], to 45.3 GPa using the FP-LMTO approach, the LSDA and the 4f-core model [13]. This demonstrates a pronounced sensitivity of the bulk modulus to the change of the exchange–correlation functional and to the form of the crystal potential.

Finally, the expected linear increase in the exchange splitting between the 4f majority- and minority-spin states with increasing U is seen on application of the PBE + U method. Our calculated values of the exchange splitting are determined from the peak positions of the localized minority and majority 4f states in the calculated projected density of states (PDOS). XPS and BIS measurements place the occupied and unoccupied bulk 4f states at approximately -8 eV and $+4.4$ eV respectively, relative to the Fermi energy. Agreement of the calculated exchange splitting with experiment is achieved for a $(U - J)$ parameter closer to 7 eV.

All previous calculations of Gd in which the DFT + U treatment has been employed [3, 6, 15, 16, 53] are based on the LSDA and have used the Coulomb and exchange parameters of $U = 6.7$ and $J = 0.7$ eV calculated by Harmon *et al* [15]. The calculated magnetic moments lie on both sides of the experimental value: Kurz *et al* [6] find $M = 7.41$ μ_B, Shick *et al* [16] $M = 7.82$ μ_B; both used the FLAPW and the experimental lattice constant. (It should be noted that in later work on Gd(0001) surfaces, Shick *et al* [53] reported a magnetic moment of $M = 7.54$ μ_B for the central layers of their slab; the reasons for this discrepancy compared to the bulk value are not clear). In the present implementation [34] of the PBE + U method using the PBE functional, we obtain satisfactory agreement between the calculated and experimental moment for $(U - J)$ close to 6 eV (figure 1), which is consistent with the estimate of the on-site Coulomb repulsion by Harmon *et al*. Based on the results in figure 1 and the consistency with the calculated U and J parameters of Harmon *et al*, we use $U - J = 6$ eV for all further calculations. The good agreement between our optimization of $U - J$ with respect to the properties of bulk Gd, and the calculations of Harmon *et al* for the free atom emphasizes the fact that both U and J are intra-atomic properties. Hence the same value should be used in bulk and surface calculations.

3.2. Ground-state structural and magnetic properties

The variation of the total energy with atomic volume obtained using the PBE and PBE + U methods is shown in figure 2 for both the ferromagnetic (FM) and antiferromagnetic (AFM) states. We reproduce the well-documented (incorrect) favouring of the AFM ground state in our PBE calculations, with the 4f electrons treated as band states. Jenkins *et al* [14] similarly found that the PBE functional favours the AFM ground state in their FP-LMTO calculations in which the 4f electrons were treated as itinerant band states, although they obtained the correct FM ground state when using the LMTO-ASA method instead. We note that in our calculations,

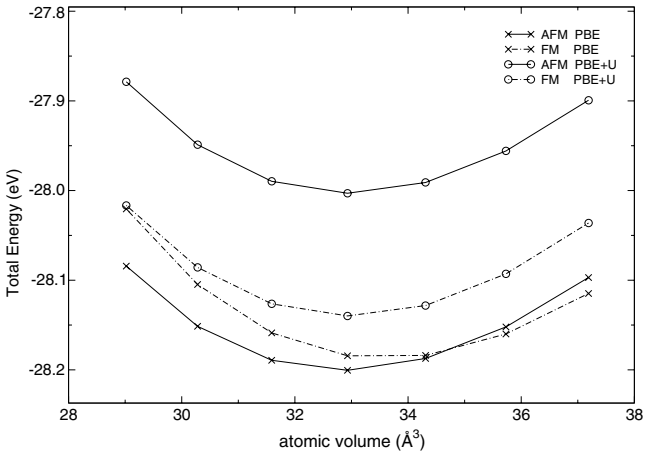

Figure 2. Energy variation with hcp unit cell volume per atom for the antiferromagnetic (solid curves) and ferromagnetic states (dashed curves) calculated with the PBE (×) and PBE + U (○) methods.

the c/a ratio is relaxed at each volume to obtain the total energy curves in figure 2, whereas Jenkins *et al* [14] performed their calculations with c/a fixed at the experimental value of 1.597. Both Eriksson *et al* [13] and Kurz *et al* [6] observed that the application of the GGA in the form of the PW91 functional only succeeds in reversing the favouring of the AFM state when the 4f electrons are treated as core rather than band states. The failure of the GGA to correctly predict the magnetic ground state of Gd is borne out in the present calculations. Only at an expanded atomic volume do PBE calculations predict the FM phase to be lower in energy than the AFM state, in agreement with the 4f-band calculations of Eriksson *et al*.

In the case of the PBE $+U$ calculations, the energetic preference for the FM ground state is restored (figure 2), in agreement with experiment. This is consistent with previous calculations performed within the LDA + U framework, in which the addition of the strong on-site intra-atomic Coulomb repulsion U between the localized 4f electrons to the DFT Hamiltonian led to the correct FM ground state [6, 15, 16]. The structural and magnetic properties obtained at the respective equilibrium volumes calculated using the PBE and PBE + U methods are summarized in table 1.

For the ferromagnetic state, the PBE functional leads to an overestimation of the lattice constant relative to experiment by 0.58% (table 1). Application of the on-site Hubbard corrections shifts the calculated equilibrium volume in the direction of experiment, and results in a and c lattice parameters that fall within 0.25% of the experimental values determined at 106 K. The corrections for strong correlations also significantly improve the agreement of the calculated magnetic moment with experiment—here it is important to realize that even small changes in the induced moment of the s, d valence electrons can lead to a significant modification of the exchange coupling. For the FM phase we find a magnetic moment of 7.44 μ_B in our PBE calculations and of 7.64 μ_B using PBE + U—the latter value is in near perfect agreement with experiment. The decomposition of the local magnetic moments into contributions from states with different angular momentum suggests that most of the increase in the total magnetic moment going from the PBE to the PBE + U case for the ferromagnetic system arises from the increase in the 4f moment, with a smaller contribution arising from the d states. In the PBE + U we also note a quite significant magnetostructural effect: while in the

FM phase the calculated axial ratio $c/a = 1.60$ is in almost perfect agreement with experiment, the interlayer distances are expanded to $c/a = 1.65$ if AFM ordering is imposed.

It is interesting to compare our results with earlier calculations at the LSDA + U level. Kurz *et al* [6] report an equilibrium lattice constant which is −2.7% smaller than experiment (no optimization of the cell geometry has been performed) and a magnetic moment in the muffin-tin spheres of 7.39 μ_B (in principle, a contribution from the interstitial region has to be added, but this information is not provided for the relaxed lattice constant). The comparison with our PBE-GGA results shows that even at the DFT + U level the gradient corrections are important for curing the overbinding characteristic for the LSDA and to stabilize magnetism. For the magnetic energy difference $\Delta E(\text{AFM} - \text{FM})$ the value of 34 meV/atom reported by Kurz *et al* [6] is only half as large as our value of 69 meV/atom which agrees very well with the result of 63 meV/atom obtained by Shick *et al* [16, 53] and the energy difference of 56 meV/atom reported by Harmon *et al* [15] using the experimental crystal structure. The existing discrepancies are likely to be attributed to different implementations of the DFT + U method. (i) We used a GGA + U approach; the earlier calculations have been performed at the LSDA + U level. (ii) For the construction of the DFT + U Hamiltonian, we followed the approach of Dudarev *et al* [34], while Kurz *et al* followed Anisimov *et al* [31] and Shick *et al* used a similar formulation proposed by Liechtenstein *et al* [33] (see also Shick *et al* [16]). We also refer to our comments on the differences of the implementations in the PAW and FLAPW formalisms, and on the influence of the choice of different muffin-tin radii in FLAPW-DFT + U calculations.

Calculations using the 4f-core model and GGA functionals agree on a magnetic energy difference of $\Delta E(\text{AFM} - \text{FM}) = 55$ meV/atom if a full potential approach is used (Kurz *et al* [6], Turek *et al* [23]—FLAPW; Eriksson *et al* [13]—FP-LMTO), while the atomic-sphere approximation reduces the energy difference to 40 meV/atom (Turek *et al* [23]—LMTO-ASA).

If the magnetic energy difference is used to estimate the strength of the exchange coupling in a nearest-neighbour Heisenberg model, and using a mean-field model for the calculation of the Curie temperature, i.e.

$$T_C^{MF} = 2\frac{\Delta E(\text{AFM} - \text{FM})}{3k_B}, \tag{5}$$

we find a significant overestimation of $T_C^{MF} = 534$ K compared to the experimental value of 293 K. We think that this result does not invalidate the PBE + U approach since (i) mean-field calculations always overestimate T_C, and (ii) due to the long-range oscillatory nature of the exchange interactions the true on-site exchange interaction will be smaller than the oversimplified nearest-neighbour estimate.

3.3. Ground-state electronic properties

The calculated band structure of Gd, determined using the PBE functional and the PBE + U method, is shown in figure 3. The shift in the 4f states away from the Fermi level induced by the on-site Coulomb repulsion, is immediately apparent. The exchange splitting of the 4f states is increased from 5.3 eV using the PBE functional to 11.3 eV with the PBE + U method, as is evident in the calculated density of states, shown in figure 4, where the projection onto the majority and minority 4f states is indicated by the shaded peaks. In the PBE results the majority-spin 4f peak is found at approximately 4.8 eV below E_F, and the minority-spin 4f peaks at 0.5 eV above E_F. This is comparable to the positions of the majority- and minority-spin manifolds obtained in previous studies using the 4f-band model and the LSDA [2–8] which place the majority 4f states at 4.5 eV below E_F. A downshift in energy of the majority-spin 4f states by 0.2 eV relative to the LSDA results was noted by Kurz *et al* [6] on application of the

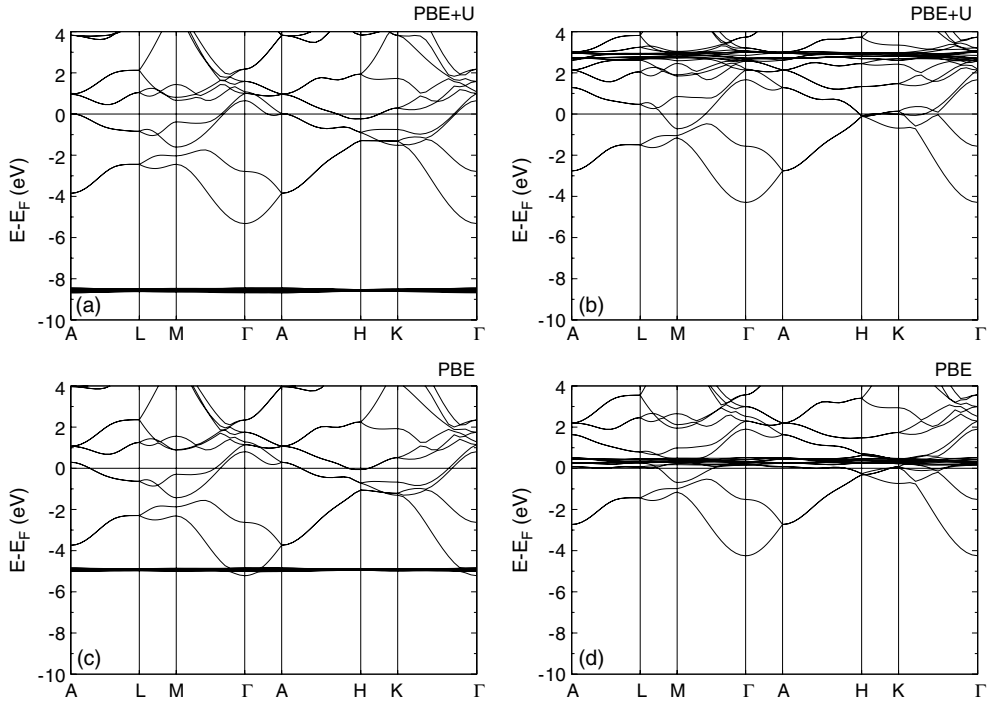

Figure 3. Calculated band structure for ferromagnetic bulk hcp Gd using the PBE + U formalism (above) and the PBE functional (below). Majority-spin states (a), and minority-spin states (b) for the PBE + U method; majority-spin states (c) and minority-spin states (d) for the PBE functional.

GGA (PW91 functional) when treating the 4f electrons as valence states. This is consistent with the present results, which similarly place the majority-spin manifold at an increased binding energy of 4.8 eV, compared to the LSDA studies.

On application of the PBE + U approach, the 4f majority-spin manifold is shifted down by about 3.6 eV to the higher binding energy of 8.4 eV relative to E_F, and the minority states are raised by 2.4–2.9 eV above E_F. From XPS and BIS measurements [9] the minimum energy required to excite a 4f electron to the Fermi level is 7.44 ± 0.1 eV, and the minimum energy to raise an electron from E_F to an unoccupied 4f level is 4.04 ± 0.2 eV. Ortega *et al* [10] similarly observed the bulk 4f core level positions at 8.05 ± 0.1 and 4.35 ± 0.1 eV, below and above E_F respectively. Thus, application of the PBE+U method brings the calculated energetic positions of the 4f manifolds into better agreement with experiment. This is in accord with previous LSDA + U calculations [6, 15, 16], for which similar shifts in the majority- and minority-spin 4f manifolds were observed. However, we note that Shick *et al* [16] obtained a slightly larger downshift of 4.5 eV for their majority 4f states, and a smaller upward shift of 1.5 eV for the minority-spin manifold using the LDA + U than we obtain here. Better agreement exists with the LDA + U results of Kurz *et al* which reported down/up-shifts of 3.8 and 1.9 eV for the 4f majority/minority states.

The exchange splitting of the Δ_2 valence band of Gd has also been measured in detail using spin- and angle-resolved photoemission spectroscopy [37, 38, 46]. In figure 3, the Δ_2 band is the first occupied band below E_F at the Γ-point. Within the PBE + U formalism, the majority $\Delta_{2\uparrow}$ band is found at 2.8 eV below E_F and the minority $\Delta_{2\downarrow}$ band at 1.6 eV below E_F at Γ, resulting in an exchange splitting of 1.2 eV. Experimentally, the exchange splitting is

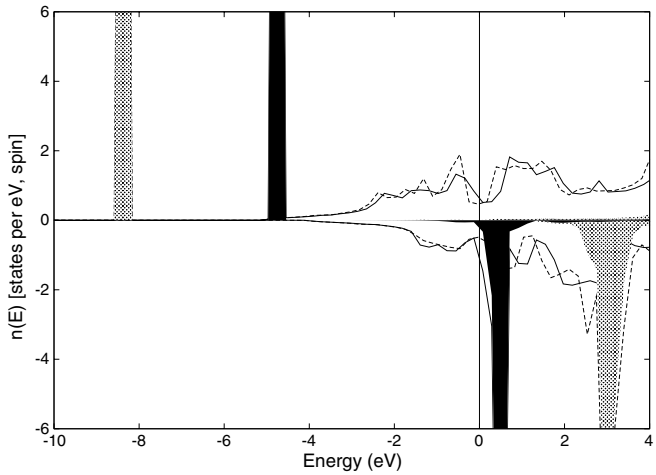

Figure 4. Spin-projected density of states for ferromagnetic bulk hcp Gd obtained with the PBE functional (solid curve) and the PBE + U method (dashed curve). The projection onto the 4f states is indicated by the light (dark) shading for the PBE + U (PBE) methods. The shift of the localized majority and minority 4f states away from the Fermi level on application of the PBE + U method is clearly seen. The majority-spin (minority-spin) densities of states are indicated by positive (negative) values of the DOS.

$\sim$0.85 $\pm$ 0.2 eV at 80 K, with the majority and minority Δ_2 peaks at approximately 2.4 and 1.6 eV, as determined with spin-polarized photoemission spectroscopy [37, 38, 46]. We note, however, that the exchange splitting is observed to be temperature dependent, increasing with decreasing temperature [37]. Examination of the projected band structure reveals that the Δ_2 band has significant d and s character, and hence can be considered to be an s–d hybridized band. Within the PBE formalism, the $\Delta_{2\uparrow}$ and $\Delta_{2\downarrow}$ bands are located at 2.6 and 1.5 eV below E_F at the Γ-point. Thus, the calculated exchange splitting is slightly less than for the PBE + U method, and the peaks are unevenly shifted to slightly lower binding energies, closer to E_F. We note that Kurz *et al* [6] calculated the $\Delta_{2\uparrow}$ and $\Delta_{2\downarrow}$ bands at 2.4 and 1.4 eV below the Fermi energy using the LSDA and the 4f-band model. If the 4f-core model is used, both states are down-shifted by about 0.2 eV. Replacing the LSDA by the GGA leads to only minimal changes in the valence bands. No information on the LSDA + U band structure is given.

Finally, we focus on the second occupied band below the Fermi energy at Γ (figure 3). This band shows pure s character. The calculated exchange splitting at Γ for this s band is 1.0 eV. The majority-spin state is shifted down by only 0.1 eV in the PBE + U calculations relative to the PBE approach, with the minority-spin state differing by a negligible 0.03 eV between the two methods.

4. Gd(0001) surface

The structural and magnetic properties of the clean Gd(0001) surface have been investigated using both the PBE and PBE + U methods. The value of ($U - J$) obtained by fitting to the bulk properties was assumed to be unchanged at the free surface. The surface was represented by a periodically repeated symmetric eight-layer slab separated by a thick vacuum region ($\sim$17 Å). The vertical positions of the top two layers on each side of the slab have been relaxed. Very similar results have been obtained for an asymmetrically relaxed six-layer slab (bottom four layers frozen). Small differences affect only the relaxation of the subsurface layer. The optimized interlayer distances and the layer-resolved magnetic moments are reported in table 2.

Table 2. Calculated relaxations $\Delta d_{i,i+1}$ of the interlayer distances and layer-resolved magnetic moments at a clean Gd(0001) surface. The magnetic moments of the surface and subsurface atoms are denoted by M_s and M_{s-1}, respectively, and the bulk moment is denoted by M_b (all moments are given in μ_B).

Method	Δd_{12} (Å)	Δd_{12} (%)	Δd_{23} (Å)	Δd_{23} (%)	M_s	M_{s-1}	M_b
PBE + U	−0.14	−4.9	+0.01	+0.5	7.88	7.66	7.63
PBE	−0.15	−5.1	+0.02	+0.6	7.46	7.36	7.41
Expt. [50]	−0.12	−4.2	+0.03	+1.0			
Expt. [51]	-0.10 ± 0.03	-3.5 ± 1.0	$+0.06 \pm 0.03$	$+2.0 \pm 1.0$			

4.1. Surface structure

The PBE + U calculations predict an inward relaxation of the surface layer by −4.9%, and an expansion of the distance between the subsurface layer and the fixed bulk-like layers by +0.5%. A PBE calculation leads to marginally larger displacement amplitudes. The PBE + U results lie slightly outside the LEED data of Quinn *et al* [51]; slightly larger relaxations of the surface layer have been reported by Giergiel *et al* [50]. LSDA calculations using the 4f-band(core) model yield an inward relaxation of −3.0(−2.9)%, increasing to −3.5% if gradient corrections are added [6]. However, in these calculations, only the top layer has been allowed to relax. No previous optimizations of the surface structure based on a DFT + U approach are known.

4.2. Magnetic properties and phase transition

The PBE calculations predict only a very modest surface-induced enhancement of the magnetic moments by 0.05 μ_B, and even a slight reduction of the moments carried by the atoms in the subsurface (see table 2). In contrast the PBE + U method predicts an increase of the magnetic moment from 7.63 μ_B for the bulk atoms to 7.88 μ_B for the surface atoms. The surface-induced enhancement is due largely to an increased magnetic polarization of the d-valence states, whose contribution to the magnetic moment increases from 0.49 μ_B in the bulk to 0.71 μ_B at the free surface, while the s-electron contribution increases from 0.08 to 0.12 μ_B only. A similar enhancement is reported in the LSDA + U work of Shick *et al* [53]. No enhanced moments are found in LSDA calculations using the 4f-band model, while the 4f-core model leads to a modest surface-induced enhancement by about 0.1 μ_B [6, 13].

The most striking experimental observation on the Gd(0001) surface is the existence of a magnetic transition at the surface at a higher Curie temperature than in bulk Gd, $T_C^s > T_C$. The nature of the phase transitions at the surface of magnetic materials and in thin magnetic films has been studied repeatedly in the past [82–85]. The main aim of these studies was to determine under which conditions a magnetic surface phase transition decoupled from the magnetic transition in the bulk is possible. The earliest studies in this direction were performed by Binder and Hohenberg [82], who demonstrated that in Ising and Heisenberg systems with different nearest-neighbour coupling in the bulk and at the surface, distinct phase transitions can occur at the surface and in the bulk. Later extensive Monte Carlo calculations for semi-infinite three-dimensional Ising models have been used to establish the phase diagram for a material where the exchange interaction J_s at the surface differs from that in the bulk [83]. It has been shown that a surface phase transition decoupled from the phase transition in the bulk can occur in two different regimes. (a) $J_b > 0$ and $J_s < 0$. Here the bulk is ferromagnetically ordered below a bulk critical temperature T_{cb}, and the interface orders antiferromagnetically at a temperature T_{cs}. (b) $J_b > 0$ and $J_s > J_b$. If the exchange coupling at the surface is much stronger than in the bulk, the surface remains ferromagnetically ordered above T_C and the surface phase transition

shows two-dimensional critical behaviour. At $J_s \simeq 1.52\ J_b$ the bulk and surface become simultaneously critical and the phase boundaries meet at a new multicritical point. Spišák and Hafner [85] have used *ab initio* DFT calculations of the exchange coupling in combination with Monte Carlo simulations on an Ising model to investigate magnetic phase transitions in thin Fe/Cu(100) films. It was demonstrated that the surface-induced enhancement of magnetism at the free surface was strong enough to decouple the paramagnetic to ferromagnetic transition at the surface from that in the deeper layers of the film. However, it was also pointed out that while simulations based on short-range exchange interactions are sufficient to determine the relative magnitude of the Curie temperatures, reliable absolute values can be achieved only using the full long-range exchange interactions. These restrictions must be remembered in the following.

A molecular-field approach to a semi-infinite Heisenberg system was developed by Mills [86] and recently adapted by Shick *et al* [53] to study the Gd(0001) surface. If the ratio of the nearest-neighbour exchange coupling in the bulk and at the surface satisfies

$$1.5 - 2\frac{J_b}{J_s} \geqslant 0, \tag{6}$$

the static magnetic susceptibility has two poles corresponding to the bulk and surface Curie temperatures which are related by

$$T_C^s = \left[1 + \left(1.5 - 2\frac{J_b}{J_s}\right)^2\right] \times T_C. \tag{7}$$

To determine the exchange coupling ratio at the bulk and at the surface, we have calculated the energy difference between the completely FM Gd(0001) slab and a slab in which the magnetic moments in the surface layer are antiparallel to those in the bulk (in the following we use the notation $\uparrow\uparrow$ and $\downarrow\uparrow$ for both surface configurations). The surface geometry of the $\downarrow\uparrow$ phase was relaxed independently, and as expected from the geometries of the FM and AFM phases (see table 1), a reduced inward relaxation of $\Delta d_{12} = -1.4\%$ was found. The energy difference $\Delta E(\downarrow\uparrow - \uparrow\uparrow)$ calculated using the PBE + U approach is 133 meV/surface-atom, i.e. nearly twice as large as the AFM/FM energy difference in the bulk. If, following Shick *et al*, we approximate the exchange coupling ratio by

$$\frac{J_s}{J_b} \sim \frac{\Delta E(\downarrow\uparrow - \uparrow\uparrow)}{\Delta E(\mathrm{AFM} - \mathrm{FM})} = 1.93 \tag{8}$$

and use the mean-field expression for the Curie temperatures, we find a surface Curie temperature enhanced by 21%, in reasonable agreement with the 29% enhancement found in the experiment [44]. This result also agrees with the LSDA + U calculations of Shick *et al*, who reported an exchange-coupling ratio of $J_s/J_b = 2.14$, corresponding to $T_C^s = 1.33 \times T_C$. However, their calculations were performed for a fixed surface geometry, with the interlayer distances taken from the LEED experiments of Giergiel *et al* [50]. The more pronounced enhancement compared to our calculations is due to the fact that no independent relaxation of the $\downarrow\uparrow$ configuration was allowed. For a bulk-terminated surface, Shick *et al* calculate an exchange-coupling ratio of $J_s/J_b = 1.14$ and hence no surface phase transition. Their conclusion was that the enhancement of the Curie temperature at the surface is induced by the inward relaxation of the top layer. The LSDA + U calculations of Kurz *et al* [6] yield a rather dramatic enhancement of both the exchange coupling and the Curie temperature, $J_s/J_b = 2.79(2.54)$ and $T_C^s = 1.61(1.51) \times T_C$, for relaxed (unrelaxed) surfaces. The difference compared to the results of Shick *et al* and to those reported here is due almost entirely to a much smaller magnetic energy difference in the bulk (see the discussion above). Calculations using the LSDA and the 4f-core model lead to weaker surface effects ($J_s/J_b = 1.93(1.78)$ and $T_C^s = 1.21(1.14) \times T_C$, for relaxed (unrelaxed) surfaces) which are closer to our PBE + U results.

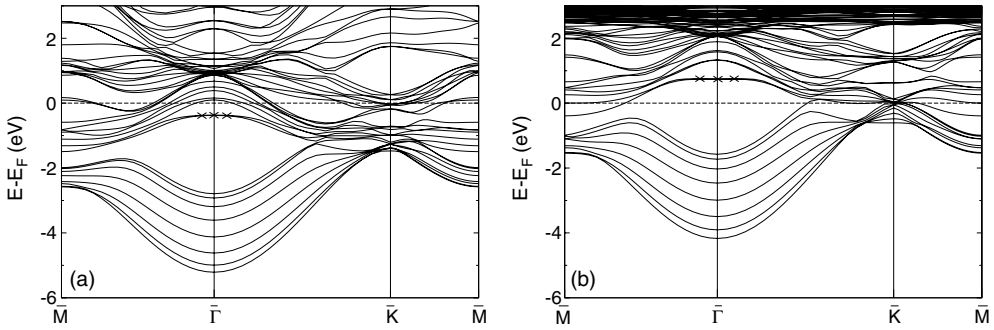

Figure 5. Spin-resolved surface band structure for Gd(0001). (a) Majority-spin states, (b) minority-spin states. The occupied surface state at −0.37 eV and the unoccupied state at +0.74 eV at $\overline{\Gamma}$ are indicated by the × symbols.

4.3. Electronic properties

The most thoroughly investigated feature of the surface electronic structure of Gd(0001) is the spin-split surface state around Γ (the Δ_2-state) formed in the large gap of the projected electronic structure of the bulk which has been probed by photoemission [87] and scanning-tunnelling [88] spectroscopies. Experimentally, the majority component of the surface state has been located at −0.20 to −0.25 eV, and the minority component at ∼0.40–0.50 eV relative to the Fermi level. The state of the art of theoretical investigations of the surface state has been summarized by Kurz *et al* [6]. Calculations using the LSDA 4f-core model place the majority and minority surface states at −0.24 eV below and 0.95 eV above E_F; the corresponding results of LSDA + U calculations are −0.22 and 0.92 eV. Differences between bulk-terminated and relaxed surfaces are quite insignificant: they never exceed 0.03 eV. The spin-resolved band structure for Gd(0001) from our GGA + U calculations is shown in figure 5. We find the majority component of the surface state at −0.37 eV and the minority component at +0.74 eV. The splitting is thus the same as that reported by Shick *et al* [53], although both our peaks are shifted down in energy by 0.2 eV relative to theirs as an effect of using the GGA. This downshift effect on replacing the LSDA by the GGA was also noted by Kurz for the bulk band structure; see the discussion in section 3.3.

For the 4f states, surface-induced shifts of the empty 4f minority states and of the occupied 4f majority states by $\delta_s(\downarrow) = -0.30$ eV and $\delta_s(\uparrow) = -0.32$ eV to lower energies (compared to the band positions in the centre of the slab) have been calculated. This is in good agreement with the IPES and PES experiments of Fedorov *et al* [89] finding shifts of $\delta_s(\downarrow) = -0.48 \pm 0.04$ eV and $\delta_s(\uparrow) = -0.29 \pm 0.03$ eV for minority and majority states, respectively. Previously, LSDA and LSDA + U calculations of the surface shifts of the 4f states have been presented by Sabiryanov and Jaswal [3]. While LSDA calculations based on the LMTO-ASA approach predict only a modest shift of −0.15 eV for both majority and minority states (which are only marginally enhanced to −0.23 eV if an FP-LMTO approach is used), the LSDA + U calculations in the LMTO-ASA produce a larger shift in agreement with experiment.

We have also calculated the work function of the Gd(0001) surface. Our PBE + U result of $\Phi = 3.47$ eV agrees quite well with the experimental value of 3.3 ± 0.1 eV [90, 91]. The LSDA calculations of Eriksson *et al* [13] using the 4f-core model led to a significantly lower value of $\Phi = 2.91$ eV.

Table 3. Relative energy, structural and magnetic properties for H adsorption on Gd(0001) at a coverage of 0.25 ML. d_{rad} denotes the radial displacement of the surrounding Gd surface atoms towards the H atom, and d_{vert} the maximum downward displacement (indicated by negative values) in the surface layer, relative to the clean surface. M_{GdH} and M_{Gd} denote the magnetic moments on the Gd atoms bonded and not bonded to the H atom in the surface layer, respectively.

Site	ΔE (eV)	$d_{\mathrm{Gd-H}}$ (Å)	d_{rad} (Å)	d_{vert} (Å)	M_{GdH} (μ_{B})	M_{Gd} (μ_{B})
fcc	0.00	2.28	0.06	−0.10	7.74	7.83
hcp	0.06	2.26	0.10	−0.05	7.73	7.83
Bridge	0.34	2.20	—	—	7.72	7.81
Top	1.31	2.09	—	−0.05	7.53	7.75

5. Hydrogen adsorption on Gd(0001)

To study the change in the surface properties induced by the adsorption of hydrogen, we have used a (2 × 2) supercell containing a single H atom, corresponding to a coverage of 0.25 monolayers (ML). We have compared adsorption in four different high-symmetry sites (on-top, bridge, fcc and hcp hollows), allowing the adsorbate and the atoms in the two top layers of a six-layer slab to relax to their optimal positions. In addition, we have determined the energy profile for the migration of H atoms into subsurface sites.

5.1. Adsorption energetics and geometry

A summary of the adsorption geometries, the relative adsorption energies, and the magnetic moments of the Gd surface atoms as calculated using the above methodology is compiled in table 3. The most stable adsorption site is the fcc hollow, with an adsorption energy (relative to molecular hydrogen in the gas phase) of $E_{\mathrm{ads}} = 0.92$ eV/H atom. The site assignment agrees with the analysis of Li *et al* [55]. The energy difference between the fcc and hcp hollows is only 60 meV; the bridge site represents a saddle-point on the potential-energy surface. The energy difference of $\Delta E = 0.34$ eV corresponds to the activation energy for H diffusion on the Gd surface; this low-energy barrier shows that hydrogen is a rather mobile species on this surface. Adsorption on top of a Gd atom is strongly disfavoured. H adsorption induces a slight corrugation of the surface. For both three-fold sites, the surface Gd atoms bonded to the adsorbate move radially inwards towards the adsorption site, while the remaining bare surface Gd atom responds by shifting inwards towards the second layer (by −0.10 Å for the fcc geometry and −0.05 Å for the hcp case). Smaller distortions are observed in the second layer, most noticeably for the hcp site, where the Gd atom located directly below the adsorbate experiences an inward contraction by −0.08 Å.

H adsorption has a weak demagnetizing effect on the Gd surface. On the Gd sites binding to the adsorbate, the local magnetic moment is slightly reduced: the effect is strongest for on-top adsorption (with only one Gd atom binding to hydrogen), and weakest for adsorption in one of the threefold hollows. For all four sites, there is a small induced moment of −0.010 to −0.014 μ_{B} on the H atom. A reduced surface magnetization of H-covered Gd surfaces was also reported by Cerri *et al* [54] on the basis of spin-polarized photoemission studies.

5.2. Diffusion of hydrogen into subsurface sites

The energy profile for the diffusion of H atoms from the fcc site into subsurface sites was calculated by incrementally fixing the vertical position of the atom, while relaxing the positions of the surrounding atoms. The calculated profile shown in figure 6 yields an energy barrier of

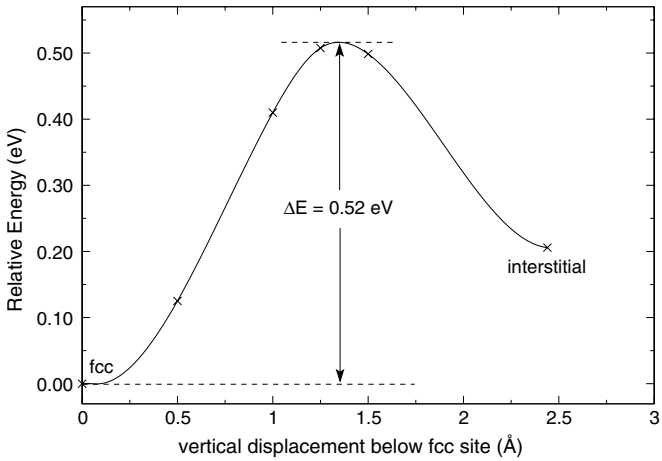

Figure 6. Energy profile for H diffusion from the fcc site to the interstitial site, with a calculated barrier to diffusion of 0.52 eV. Points corresponding to calculated geometries are indicated by the × symbol, with the interpolated curve being a guide to the eye only.

0.52 eV. This value is compatible with the onset of diffusion into the bulk at $T \geqslant 195$ K, as reported in [55].

5.3. Electronic structure

The projected density of states for a hydrogen-covered Gd(0001) surface at 0.25 ML is shown in figure 7(a); the DOS for H in subsurface sites is shown in part (b) of this figure. The most prominent features are the spin-polarized H-induced states below the bottom of the valence band. For H in the fcc hollows, the H s states hybridize strongly with the 5d states on the nearest neighbour Gd sites; the majority and minority components of the bonding H s–Gd 5d states are located at binding energies of −4.6 and −4.1 eV, respectively. Antibonding H s–Gd 5d states at lower binding energy merge with the bulk band and are not distinctly visible in the DOS. For H in subsurface positions, bonding H s–Gd 5d states are found at −5.8 and −5.2 eV, respectively.

To investigate the H-induced states further, we calculated the band structure of the Gd(0001) surface with an increased coverage of 1 ML of hydrogen adsorbed in either the fcc hollows, or in the tetrahedral subsurface sites. The corresponding spin-projected band structure is shown in figure 8 for both adsorption geometries. The band-structure allows to identify a bonding H s–Gd 5d state located below the bottom of the projected bulk bands and extending over the entire Brillouin zone, and around $\overline{\Gamma}$ an antibonding H s–Gd 5d state in the gap between the bulk bands. Compared to lower H coverage the dispersion of these states is increased. For H adsorbed in the fcc hollow sites, the majority component of the bonding H-induced state disperses between −6 eV at $\overline{\Gamma}$ and −4.1 eV at $\overline{K}$, and the minority component between −5.3 and −3.7 eV. The majority component of the antibonding H-induced state at $\overline{\Gamma}$ lies at −1.0 eV; towards the surface of the Brillouin zone the downward dispersing band merges with bulk states, and the exchange splitting pushes the minority components at $\overline{\Gamma}$ above the Fermi level. For H in subsurface sites, the bonding–antibonding splitting is increased, pushing the bonding state farther below the bottom of the bulk bands; the minority component of the antibonding band is now also fully occupied. For H adsorption in the fcc hollow, the Δ_2 surface state is suppressed, while it reappears for subsurface hydrogen.

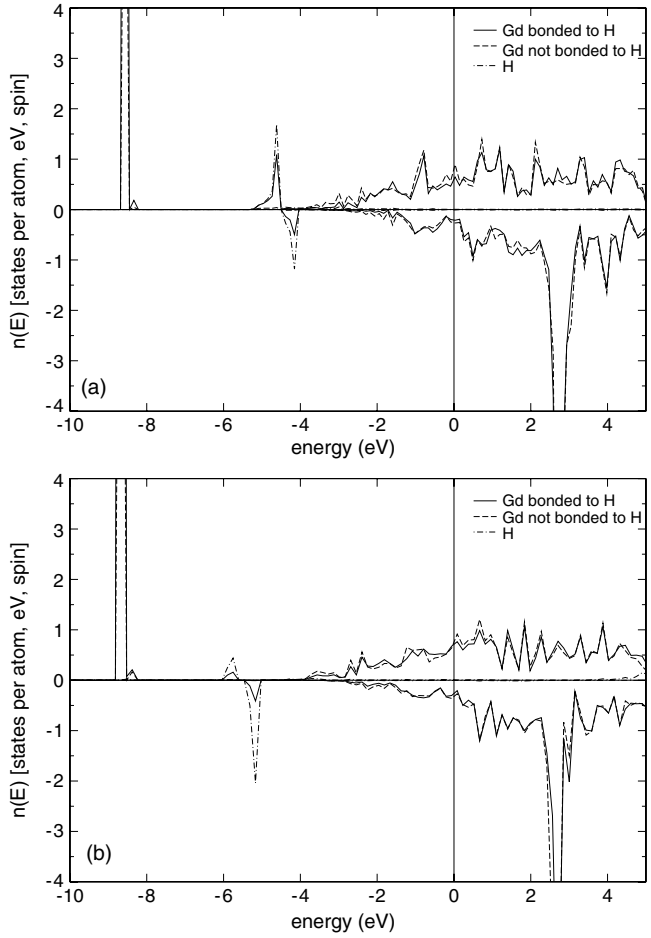

Figure 7. Projected densities of states for a H-covered Gd(0001) surface (fcc site) (a) and the same surface with H in tetrahedral subsurface positions (b). The coverage is 0.25 ML. The DOS is shown for H sites; for Gd surface atoms we differentiate between sites forming bonds to H atoms or not.

Our results for H-induced states on Gd(0001) are in very good agreement with previous investigations of hydrogen adsorbed on close-packed transition-metal surfaces, beginning with the work of Feibelman *et al* [92] on H on Ti(0001). For H on Ti(0001), the electronic structure results have been confirmed in detail by angular-resolved photoemission (PES) experiments. Unfortunately, the situation is not as clear-cut for Gd(0001). For low-temperature H adsorption at 120 K, the PES experiments of Li *et al* [55] taken at normal emission show the appearance of H-induced states at binding energies of ~ -3.8 eV whose intensity increases with increasing H exposure. Parallel to the increasing intensity of the H-induced state, the intensity of the surface state just below E_F decreases. For room-temperature adsorption the hydrogen-induced state saturates at much higher exposures. This is consistent with the fact that hydrogen starts to diffuse into the bulk at $T \geqslant 195$ K. Off-normal emission spectra (adsorption temperature unknown) show two H-induced features at -6 and -4 eV, respectively, even at very low hydrogen exposures. In contrast Getzlaff *et al* [57] observed only the -4 eV feature at H exposures of up to 2 L; only at even higher exposures does a weak maximum appear at -6 eV. Li *et al* [55] interpreted the two H-induced states as a bonding/antibonding pair of hybridized H s–Gd 5d states.

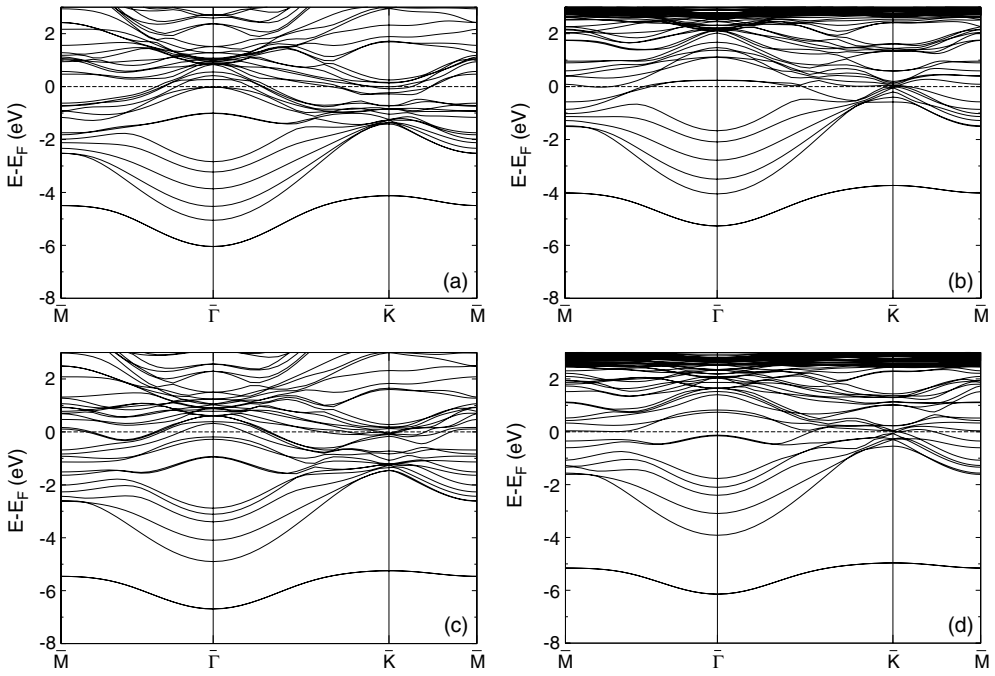

Figure 8. Spin-projected surface band structure for hydrogen adsorption on Gd(0001) at full monolayer coverage in the fcc sites (a) and (b); and in the interstitial site (c) and (d). Majority-spin states are depicted in (a) and (c), minority-spin states in (b) and (d).

Our result suggests a different interpretation. States at binding energies of about -4 eV originate from H atoms adsorbed on the surface, while the -6 eV feature has to be attributed to subsurface H. The antibonding H s–Gd 5d states cannot be seen in the PES, because they merge with the bulk bands. This interpretation is in agreement with the observation that for low-temperature adsorption ($T \sim 120$ K) the -4 eV state is always much more intense than the peak at -6 eV.

It is more difficult to reconcile our results with the angular-resolved photoemission (ARUPS) studies of Li *et al* [55]. For the H-induced state at ~ -4 eV, our results shown upward dispersion at $\overline{\Gamma}$ and downward dispersion at $\overline{K}$ and $\overline{M}$, in agreement with both theoretical and experimental results for H on Ti(0001), whereas Li *et al* report downward dispersion both at the centre and at the surface of the Brillouin zone. It is difficult to imagine the character of a state with such features. Li *et al* also report that the ARUPS spectra are at least qualitatively independent of coverage and suggest that the H atoms form islands on the Gd surface. Such an inhomogeneous H coverage is not considered in our study.

We calculate a H-induced change of the work function of $\Delta\Phi = -0.35$ eV for 1 ML of H in fcc sites and $+0.19$ eV for 1 ML of H in subsurface sites. Experimentally a decrease in the work function with coverage, up to -0.21 ± 0.05 eV at saturation, has been reported [55]. This indicates that at saturation H populates both surface and subsurface sites in thermal equilibrium.

6. Conclusions

We have presented a comprehensive investigation of the structural, electronic and magnetic properties of bulk Gd and of clean and H-covered Gd(0001) surfaces using DFT+U techniques. For bulk Gd the important result is that the combination of a gradient-corrected density-

functional approach with on-site Coulomb correction for the 4f states allows an accurate description of the geometric and electronic structures and of the magnetic properties to be achieved using a single value ($U - J = 6$ eV) of the Coulomb repulsion. It is also encouraging that this optimal value of $U - J$ agrees with the Coulomb and exchange parameters derived by Harmon *et al* [15], $U = 6.7$ eV, $J = 0.7$ eV. The PBE approach is definitely an improvement over previous studies on the LSDA + U level. An important success of the DFT + U approach is to stabilize the ferromagnetic phase, although the magnetic energy difference is found to depend quite sensitively on the details of its implementation.

For the clean Gd(0001) surface, the most widely discussed property is the magnetic surface phase transition. We show that the PBE + U approach leads to an accurate description of the surface relaxation and of the electronic surface state. We show that the magnetic exchange interaction remains ferromagnetic at the free surface, and that a surface layer coupling antiferromagnetically to the ferromagnetic substrate shows a different relaxation behaviour from the completely ferromagnetic system. If the magnetic energy differences between ferro- and antiferromagnetic coupling of the surface layer ($\Delta E(\downarrow\uparrow - \uparrow\uparrow)$) and between the ferro- and antiferromagnetic bulk phases ($\Delta E(\mathrm{AFM} - \mathrm{FM})$) are used to estimate the ratio of the exchange coupling at the surface and in the bulk, we derive, within a simple molecular-field approach, a very reasonable ratio between the surface and bulk Curie temperatures. The surface-induced enhancement of the magnetic moments and the different relaxation properties of the FM and AFM coupled surfaces are important to achieve this kind of agreement. It is important to emphasize that the 4f-core model predicts a much more modest surface-induced enhancement of the moment than the DFT + U approach. Our work is also the first to use the full PBE + U Hamiltonian for an independent relaxation of both magnetic surface configurations.

Hydrogen is adsorbed in the fcc hollows of the Gd(0001) surface, but there is a barrier of only 0.5 eV for diffusion into interstitial subsurface sites. H adsorption has a weak demagnetizing effect on the Gd surface. Adsorption on the surface leads to the formation of a band of bonding H s–Gd 5d states below the bottom of the valence band and of an antibonding H-induced state in the gap of the projected bulk bands. The occupied surface state characteristic for the clean Gd(0001) surface disappears. There is a weak exchange splitting of the bonding H-induced state and a larger splitting of the antibonding state whose minority component is only partially occupied. H in subsurface sites leads to a similar formation of a pair of bonding/antibonding H s–Gd 5s states at somewhat larger binding energies. It is essential to use the DFT + U approach for describing the adsorption properties because the bonding H-induced states lie in the gap between the s, d valence band complex and the occupied 4f states, and the antibonding H-derived states cross the Fermi level. In summary: we have demonstrated that a gradient-corrected DFT combined with a Hubbard-like description of the on-site Coulomb repulsions in the 4f band (the PBE+U method) leads to an improved description of the physical properties of Gd. This conclusion should also apply to other rare-earth systems.

Acknowledgment

This work has been supported by the Austrian Science Funds under project No 16148-NO2.

References

[1] Roeland L W, Cock G J, Muller F A, Moleman A C, McEwen K A, Jordan R G and Jones D W 1975 *J. Phys. F: Met. Phys.* **5** L233
[2] Singh D J 1991 *Phys. Rev.* B **44** 7451

[3] Sabiryanov R F and Jaswal S S 1997 *Phys. Rev.* B **55** 4117
[4] Rex S, Eyert V and Nolting W 1999 *J. Magn. Magn. Mater.* **192** 529
[5] Sticht J and Kübler J 1985 *Solid State Commun.* **53** 529
[6] Kurz P, Bihlmayer G and Blügel S 2002 *J. Phys.: Condens. Matter* **14** 6353
[7] Krutzen B C H and Springelkamp F 1989 *J. Phys.: Condens. Matter* **1** 8369
[8] Temmerman W M and Sterne P A 1990 *J. Phys.: Condens. Matter* **2** 5529
[9] Lang J K, Baer Y and Cox P A 1981 *J. Phys. F: Met. Phys.* **11** 121
[10] Ortega J E, Himpsel F J, Li D and Dowben P A 1994 *Solid State Commun.* **91** 807
[11] Heinemann M and Temmerman W M 1994 *Phys. Rev.* B **49** 4348
[12] Heinemann M and Temmerman W M 1994 *Surf. Sci.* **307–309** 1121
[13] Eriksson O, Ahuja R, Ormeci A, Trygg J, Hjortstam O, Söderlind P, Johansson B and Wills J M 1995 *Phys. Rev.* B **52** 4420
[14] Jenkins A C, Temmerman W M, Ahuja R, Eriksson O, Johansson B and Wills J 2000 *J. Phys.: Condens. Matter* **12** 10441
[15] Harmon B N, Antropov V P, Liechtenstein A I, Solovyev I V and Anisimov V I 1995 *J. Phys. Chem. Solids* **56** 1521
[16] Shick A B, Liechtenstein A I and Pickett W E 1999 *Phys. Rev.* B **60** 10763
[17] Langreth D C and Mehl M J 1983 *Phys. Rev.* B **28** 1809
[18] Hu C D and Langreth D C 1985 *Phys. Scr.* **32** 391
[19] Perdew J P, Chevary J A, Vosko S H, Jackson K A, Pederson M R and Singh D J 1992 *Phys. Rev.* B **46** 6671
[20] Perdew J P, Burke K and Ernzerhof M 1996 *Phys. Rev. Lett.* **77** 3865
[21] Richter M and Eschrig H 1989 *Solid State Commun.* **72** 263
[22] Ahuja R, Auluck S, Johansson B and Brooks M S S 1994 *Phys. Rev.* B **50** 5147
[23] Turek I, Kudrnovský J, Bihlmayer G and Blügel S 2003 *J. Phys.: Condens. Matter* **15** 2771
[24] Bylander D M and Kleinman L 1994 *Phys. Rev.* B **49** 1608
[25] Bylander D M and Kleinman L 1994 *Phys. Rev.* B **50** 1363
[26] Bylander D M and Kleinman L 1994 *Phys. Rev.* B **50** 4996
[27] Perdew J P and Zunger A 1981 *Phys. Rev.* B **23** 5048
[28] Temmerman W M, Szotek Z and Winter H 1993 *Phys. Rev.* B **47** 1184
[29] Svane A, Temmerman W M, Szotek Z, Lægsgaard J and Winter H 2000 *Int. J. Quantum Chem.* **77** 799
[30] Petit L, Svane A, Szotek Z, Strange P, Winter H and Temmerman W M 2001 *J. Phys.: Condens. Matter* **13** 8697
[31] Anisimov V I, Aryasetiawan F and Lichtenstein A I 1997 *J. Phys.: Condens. Matter* **9** 767
[32] Anisimov V I, Zaanen J and Andersen O K 1991 *Phys. Rev.* B **44** 943
[33] Liechtenstein A I, Anisimov V I and Zaanen J 1995 *Phys. Rev.* B **52** R5467
[34] Dudarev S L, Botton G A, Savrasov S Y, Humphreys C J and Sutton A P 1998 *Phys. Rev.* B **57** 1505
[35] Liechtenstein A I, Katsnelson M I, Antropov V P and Gubanov V A 1987 *J. Magn. Magn. Mater.* **67** 65
[36] Santos C, Nolting W and Eyert V 2004 *Phys. Rev.* B **69** 214412
[37] Kim B, Andrews A B, Erskine J L, Kim K J and Harmon B N 1992 *Phys. Rev. Lett.* **68** 1931
[38] Maiti K, Malagoli M C, Dallmeyer A and Carbone C 2002 *Phys. Rev. Lett.* **88** 167205
[39] Khmelevskyi S, Turek I and Mohn P 2005 *Physica* B **359** 145
[40] Rau C and Robert M 1987 *Phys. Rev. Lett.* **58** 2714
[41] Weller D, Alvarado S F, Gudat W, Schröder K and Campagna M 1985 *Phys. Rev. Lett.* **54** 1555
[42] Tang H, Weller D, Walker T G, Scott J C, Chappert C, Hopster H, Pang A W, Dessau D S and Pappas D P 1993 *Phys. Rev. Lett.* **71** 444
[43] Vescovo E, Carbone C and Rader O 1993 *Phys. Rev.* B **48** 7731
[44] Tober E D, Palomares F J, Ynzunza R X, Denecke R, Morais J, Wang Z, Bino G, Liesegang J, Hussain Z and Fadley C S 1998 *Phys. Rev. Lett.* **81** 2360
[45] Arnold C S and Pappas D P 2000 *Phys. Rev. Lett.* **85** 5202
[46] Mulhollan G A, Garrison K and Erskine J L 1992 *Phys. Rev. Lett.* **69** 3240
[47] Tang H, Walker T G, Hopster H, Pappas D P, Weller D and Scott J C 1993 *Phys. Rev.* B **47** 5047
[48] Li D, Pearson J, Bader S D, McIlroy D N, Waldfried C and Dowben P A 1995 *Phys. Rev.* B **51** 13895
[49] Popov A P and Pappas D P 1997 *Phys. Rev.* B **56** 3222
[50] Giergiel J, Pang A W, Hopster H, Guo X, Tong S Y and Weller D 1995 *Phys. Rev.* B **51** 10201
[51] Quinn J, Li Y S, Jona F and Fort D 1992 *Phys. Rev.* B **46** 9694
[52] Wu R, Li C, Freeman A J and Fu C L 1991 *Phys. Rev.* B **44** 9400
[53] Shick A B, Pickett W E and Fadley C S 2000 *Phys. Rev.* B **61** R9213
[54] Cerri A, Mauri D and Landolt M 1983 *Phys. Rev.* B **27** 6526
[55] Li D, Zhang J, Dowben P A and Onellion M 1993 *Phys. Rev.* B **48** 5612

[56] Getzlaff M, Bode M and Wiesendanger R 1998 *Surf. Sci.* **410** 189
[57] Getzlaff M, Bode M, Pascal R and Wiesendanger R 1999 *Phys. Rev.* B **59** 8195
[58] Getzlaff M, Bode M, Pascal R and Wiesendanger R 1999 *Appl. Surf. Sci.* **142** 63
[59] Kresse G and Hafner J 1993 *Phys. Rev.* B **47** 558
[60] Kresse G and Hafner J 1994 *Phys. Rev.* B **49** 14251
[61] Kresse G and Furthmüller J 1996 *Phys. Rev.* B **54** 11169
[62] Kresse G and Furthmüller J 1996 *Comput. Mater. Sci.* **6** 15
[63] Kresse G and Joubert D 1999 *Phys. Rev.* B **59** 1758
[64] Blöchl P 1994 *Phys. Rev.* B **50** 17953
[65] Ceperley D M and Alder B 1980 *Phys. Rev. Lett.* **45** 566
[66] Vosko S H, Wilk L and Nussair M 1980 *Can. J. Phys.* **58** 1200
[67] Moroni E G, Kresse G, Hafner J and Furthmüller J 1997 *Phys. Rev.* B **56** 15629
[68] Gross A, Wilke S and Scheffler M 1995 *Phys. Rev. Lett.* **75** 2718
[69] Eichler A, Hafner J, Gross A and Scheffler M 1999 *Phys. Rev.* B **59** 13297
[70] Dudarev S L, Liechtenstein A I, Castell M R, Briggs G A D and Sutton A P 1997 *Phys. Rev.* B **56** 4900
[71] Bengone O, Alounai M, Blöchl P and Hugel J 2000 *Phys. Rev.* B **62** 16392
[72] Rohrbach A, Hafner J and Kresse G 2004 *Phys. Rev.* B **69** 075413
[73] Monkhorst H J and Pack J D 1976 *Phys. Rev.* B **13** 1588
[74] Methfessel M and Paxton A T 1989 *Phys. Rev.* B **40** 3616
[75] Murnaghan F D 1944 *Proc. Natl Acad. Sci. USA* **30** 244
[76] Rollmann G, Rohrbach A, Entel P and Hafner J 2004 *Phys. Rev.* B **69** 165107
[77] Banister J, Legvold S and Spedding F H 1954 *Phys. Rev.* **94** 1140
[78] Palmer S B, Lee E W and Islam M N 1974 *Proc. R Soc.* A **338** 341
[79] Gschneidner K A and Eyring L (ed) 1978 *Handbook on the Physics and Chemistry of Rare Earths* vol 1 (Amsterdam: North-Holland) chapter 8
[80] Rosen M 1968 *Phys. Rev.* **174** 504
[81] Lide D R (ed) 2004 *CRC Handbook of Chemistry and Physics* 85th edn (New York: CRC Press)
[82] Binder K and Hohenberg P C 1972 *Phys. Rev.* B **6** 3461
[83] Landau D P and Binder K 1990 *Phys. Rev.* B **41** 4633
[84] Peczak P and Landau D P 1991 *Phys. Rev.* B **43** 1048
[85] Spišák D and Hafner J 1997 *Phys. Rev.* B **56** 2646
[86] Mills D L 1971 *Phys. Rev.* B **3** 3887
[87] Weschke E, Schüssler-Langeheine C, Meier R, Fedorov A V, Starke K, Hübinger F and Kaindl G 1996 *Phys. Rev. Lett.* **77** 3415
[88] Getzlaff M, Bode M, Heinze S, Pascal R and Wiesendanger R 1998 *J. Magn. Magn. Mater.* **184** 155
[89] Fedorov A V, Arenholz E, Starke K, Navas E, Baumgarten L, Laubschat C and Kaindl G 1994 *Phys. Rev. Lett.* **73** 601
[90] Himpsel F J and Reichl B 1983 *Phys. Rev.* B **28** 574
[91] Michaelson H B 1977 *J. Appl. Phys.* **48** 4729
[92] Feibelman P J, Hamann D R and Himpsel F J 1980 *Phys. Rev.* B **22** 1734